

ORIGINAL ARTICLE

Potent antitumor effects of bevacizumab in a microenvironment-dependent human lymphoma mouse model

F Mori¹, T Ishida¹, A Ito¹, F Sato², A Masaki¹, H Takino², M Ri¹, S Kusumoto¹, H Komatsu¹, R Ueda¹, H Inagaki² and S Iida¹

We established a mouse model of microenvironment-dependent human lymphoma, and assessed the therapeutic potential of bevacizumab, an antitumor agent acting on the microenvironment. NOD/Shi-*scid*, IL-2R γ^{null} (NOG) mice were used as recipients of primary tumor cells from a patient with diffuse large B-cell lymphoma (DLBCL), which engraft and proliferate in a microenvironment-dependent manner. The lymphoma cells could be serially transplanted in NOG mice, but could not be maintained in *in vitro* cultures. Injection of bevacizumab together with CHOP (cyclophosphamide, doxorubicin, vincristine, prednisolone) significantly increased necrosis and decreased vascularization in the tumor, compared with CHOP alone. Levels of human soluble interleukin-2 receptor (sIL2R) in the serum of bevacizumab + CHOP-treated mice (reflecting the DLBCL tumor burden) were significantly lower than in CHOP recipients. Mice receiving bevacizumab monotherapy also showed significant benefit in terms of tumor necrosis and vascularization, as well as decreased serum sIL2R concentrations. The present DLBCL model reflects the human DLBCL *in vivo* environment more appropriately than current mouse models using established tumor cell lines. This is the first report to evaluate the efficacy of bevacizumab in such a tumor microenvironment-dependent model. Bevacizumab may be a potential treatment strategy for DLBCL patients.

Blood Cancer Journal (2012) 2, e67; doi:10.1038/bcj.2012.12; published online 20 April 2012

Keywords: bevacizumab; NOD/Shi-*scid*; IL-2R γ^{null} (NOG) mouse; lymphoma; tumor microenvironment

INTRODUCTION

Tumors develop in a complex and dynamic microenvironment. Surrounding or within the tumor nests, stromal cells, endothelial cells, innate immune cells and other lymphocytes are present that interact with each other and with the tumor cells. A large body of evidence has accumulated in the past decade demonstrating that this complex tumor microenvironment regulates tumor growth, invasion, and metastasis.¹ Angiogenesis is one of the most important phenomena within the tumor microenvironment; cancer cells have the ability to recruit and generate new blood vessels through the secretion of angiogenic factors. Tumor angiogenesis ensures that cells in the interior of the tumor receive sufficient nutrients and oxygen to survive. Blocking tumor angiogenesis would therefore severely restrict tumor growth.² Early experiments using mouse xenografts indicated that antibody-mediated inhibition of vascular endothelial growth factor (VEGF), which promotes the proliferation and migration of vascular endothelial cells and vessel sprouting, could severely inhibit angiogenesis and tumor growth.³ These and other studies led to the development of the anti-VEGF neutralizing antibody bevacizumab for therapeutic use.⁴ However, a current crucial problem in the research field of anti-tumor microenvironment agents such as bevacizumab is the lack of suitable small animal models. To the best of our knowledge, all preclinical testing of the antitumor activity of bevacizumab in mice *in vivo* has been performed using established tumor cell lines, which by definition can be maintained *in vitro* in culture.

Such tumor cells have thus been selected for survival in the absence of any microenvironment, including the vascular system. Using these established lines in mouse xenograft models therefore seems less relevant for the evaluation of the antitumor activities of anti-angiogenesis agents. Hence, the first objective of the present study was to overcome this problem. We aimed to establish a mouse model in which primary tumor cells from a patient engraft and proliferate in a microenvironment-dependent manner, using NOD/Shi-*scid*, IL-2R γ^{null} (NOG) mice as recipients.^{5,6}

Bevacizumab is currently approved world-wide for the treatment of several types of solid tumors such as colorectal cancer, breast cancer, non-small cell lung cancer, renal cell cancer and glioblastoma.^{7–15} Many aspects of pathological angiogenesis have been extensively studied in many types of solid tumors. However, the precise role of these processes in pathogenesis of hematological malignancies is still under active investigation, and in this context, bevacizumab is not currently approved for the treatment of hematological malignancies in the United States, Europe, or Japan. Thus, the second aim of the present study was to evaluate the therapeutic potential of bevacizumab with or without systemic chemotherapy for hematological neoplasia, using newly established primary tumor cell-bearing NOG mice. We selected diffuse large B-cell lymphoma (DLBCL) as the target disease because this represents the most common type of malignant lymphoma and accounts for ~30–40% of all cases in adults.^{16,17}

¹Department of Medical Oncology and Immunology, Nagoya City University Graduate School of Medical Sciences, 1 Kawasumi, Mizuho-chou, Mizuho-ku, Nagoya, Aichi, Japan and ²Department of Clinical Pathology, Nagoya City University Graduate School of Medical Sciences, 1 Kawasumi, Mizuho-chou, Mizuho-ku, Nagoya, Aichi, Japan. Correspondence: Dr T Ishida, Department of Medical Oncology and Immunology, Nagoya City University Graduate School of Medical Sciences, 1 Kawasumi, Mizuho-chou, Mizuho-ku, Nagoya, Aichi 467-8601, Japan.

E-mail: itakashi@med.nagoya-cu.ac.jp

Received 17 February 2012; revised 29 February 2012; accepted 21 March 2012

MATERIALS AND METHODS

Animals

NOG mice were purchased from the Central Institute for Experimental Animals (Kanagawa, Japan) and used at 6–8 weeks of age. All of the *in vivo* experiments were performed in accordance with the United Kingdom Coordinating Committee on Cancer Research Guidelines for the Welfare of Animals in Experimental Neoplasia, Second Edition, and were approved by the Ethics Committee of the Center for Experimental Animal Science, Nagoya City University Graduate School of Medical Sciences.

Immunopathological analysis

We assessed the affected lymph nodes of 50 patients with DLBCL by immunopathology. The patients provided written informed consent in accordance with the Declaration of Helsinki, and the present study was approved by the institutional Ethics Committee of Nagoya City University Graduate School of Medical Sciences. Hematoxylin and eosin staining and immunostaining using anti-human CD20 (L26; DAKO, Glostrup, Denmark), CD25, (4C9; Novocastra, Wetzlar, Germany), CD3 (SP7; SPRING BIOSCIENCE, Pleasanton, CA, USA), VEGF-A (sc-152, rabbit polyclonal, Santa Cruz, Heidelberg, Germany), Alpha-Smooth Muscle Actin (α -SMA; 1A4; DAKO), von Willebrand Factor (Rabbit polyclonal, DAKO), CD31 (JC70A, DAKO), CD10 (56C6; Novocastra), BCL-6 (LN22; Novocastra) and MUM1/IRF4 (M-17, Santa Cruz) were performed on formalin-fixed, paraffin-embedded sections. The presence of Epstein-Barr virus encoded RNA (EBER) was examined by *in situ* hybridization using EBER Probe (Leica microsystems, Newcastle, UK) on formalin-fixed, paraffin-embedded sections. DLBCL cases were categorized into germinal center B-cell (GCB) or non-GCB phenotypes using formalin-fixed, paraffin-embedded sections according to Hans' Algorithm.¹⁸ VEGF-A expression levels were categorized according to the following formula: 3 + positive if $\geq 50\%$, 2 + positive if $< 50 \geq 30\%$, 1 + positive if $< 30 \geq 10\%$ and negative if $< 10\%$ of the DLBCL tumor cells were stained with the corresponding antibody. Nine \times 100 high-power fields (HPF) of hematoxylin and eosin tumor specimens were randomly selected and the area of tumor necrosis (%) was calculated by Image J software¹⁹ and then averaged. Nine \times 100 HPF of von Willebrand Factor-stained tumor specimens were randomly selected and the numbers of vessels (per mm²) were calculated by Image J software¹⁹ and then averaged.

Primary DLBCL cell-bearing mouse model

The affected lymph node cells from a patient with DLBCL were suspended in RPMI-1640. The tumor cell donor provided written informed consent before sampling in accordance with the Declaration of Helsinki, and the present study was approved by the institutional Ethics Committee of Nagoya City University Graduate School of Medical Sciences. CD3-negative subsets were isolated using anti-human CD3 microbeads (Miltenyi Biotec, Bergisch Gladbach, Germany) and the autoMACS Pro Separator (Miltenyi Biotec) according to the manufacturer's instructions. Immunopathological analysis of the patient's affected lymph node revealed that the DLBCL type was non-GCB (CD10⁻, BCL-6⁻ and MUM1/IRF4⁺), and VEGF expression was 1 + positive. Six to 8 weeks after intraperitoneal (i.p.) injection, NOG mice presented with i.p. masses and splenomegaly. Cells from these i.p. masses were suspended in RPMI-1640 and i.p. inoculated into other NOG mice, which then presented with features identical to those of the first mice.

DLBCL cell lines

DB and HT were purchased from DSMZ (Braunschweig, Germany). KARPAS422, OCI-LY19, Farage, Toledo, Pfeiffer and RL were purchased from ATCC (Manassas, VA, USA).

Quantitative reverse transcription PCR

Total RNA was isolated with RNeasy Mini Kit (QIAGEN, Tokyo, Japan). Reverse transcription from the RNA to first strand cDNA was carried out using High Capacity RNA-to-cDNA Kit (Applied Biosystems Inc., Foster City, CA, USA) according to the manufacturer's instructions. Human VEGF-A (Hs00900055_m1), VEGF-R1 (Hs00176573_m1), VEGF-R2 (Hs00911700_m1) and β -actin (Hs99999903_m1) mRNA were amplified using TaqMan Gene Expression Assays with the aid of an Applied Biosystems StepOnePlus according to the manufacturer's instructions. The quantitative assessment of the mRNA of interest was done by dividing its level by that of β -actin and expressing the result relative to Human Testis Total RNA (Clontech,

Mountain View, CA, USA) as 1.0. All expressed values were averages of triplicate experiments.

Monoclonal antibodies and flow cytometry

The following monoclonal antibodies (mAbs) were used for flow cytometry: MultiTEST CD3 (clone SK7) FITC/CD16 (B73.1) + CD56 (NCAM 16.2) PE/CD45 (2D1), PerCP/CD19 (SJ25C1) APC Reagent (BD Biosciences, San Jose, CA, USA), PerCP-conjugated anti-human CD45 mAb (2D1, BD Biosciences), APC-conjugated anti-CD19 mAb (HIB19, BD Biosciences), PE-conjugated anti-CD25 mAb (M-A251, BD Biosciences), PE-conjugated VEGF-R1 mAb (49560, BD Biosciences), PE-conjugated VEGF-R2 mAb (89106, R&D Systems Inc., Minneapolis, MN, USA) and the appropriate isotype control mAbs. Whole blood cells from mice were treated with BD FACS lysing solution (BD Biosciences) for lysing red blood cells. Cells were analyzed by a FACSCalibur (BD Biosciences) with the aid of FlowJo software (Tree Star Inc., Ashland, OR, USA).

Cell proliferation assay

Proliferation of the DLBCL cell lines, which express both VEGF-A and VEGF-R in the presence of different concentrations of bevacizumab for 48 h, was assessed using the CellTiter 96 Aqueous One Solution cell proliferation assay kit (Promega Corporation, Madison, WI, USA) as described previously.²⁰ Proliferation of the NOG DLBCL cells with or without human interleukin-2 at a final concentration of 100 IU/ml was also assessed in the same manner.

Primary DLBCL cell-bearing mice treated with CHOP + bevacizumab

Tumor cells from the i.p. masses were suspended in RPMI-1640, and 1.0×10^7 were i.p. inoculated into each of 10 NOG mice. The mice were divided into two groups of five each for treatment with bevacizumab + CHOP (cyclophosphamide, doxorubicin, vincristine, prednisolone) or CHOP alone, 2 days after tumor inoculation. Bevacizumab (10 mg/kg) or control (saline) was i.p. injected into the mice 2, 9, 16, 23, 30, 37 and 44 days after tumor cell inoculations. CHOP was given i.p. 30 days after tumor inoculations at doses as follows: cyclophosphamide, 40 mg/kg; doxorubicin, 3.3 mg/kg; vincristine, 0.5 mg/kg; prednisolone, 0.2 mg/kg.²¹ Therapeutic efficacies were evaluated 49 days after tumor inoculation. Bevacizumab was purchased from Chugai Pharmaceutical Co., Ltd, Tokyo, Japan; cyclophosphamide and vincristine were purchased from Shionogi Pharmaceutical Co., Ltd, Osaka, Japan; doxorubicin was from Kyowa Hakkō Kirin Co., Ltd, Tokyo, Japan and prednisolone was from Nippon Kayaku Co., Ltd, Tokyo, Japan.

Primary DLBCL cell-bearing mice treated with bevacizumab

A total of 1.0×10^7 tumor cells were i.p. inoculated into each of 18 NOG mice, divided into two groups of nine each for bevacizumab or control. Bevacizumab (10 mg/kg) or control (saline) was i.p. injected into the mice after 3, 10, 17, 24, 31, 38 and 45 days, and therapeutic efficacies were evaluated 47 days after tumor inoculations.

Human sIL2R measurement

The concentration of human soluble interleukin-2 receptor (sIL2R) in mouse serum was measured by enzyme-linked immunosorbent assay using the human sIL2R immunoassay kit (R&D Systems, Inc.) according to the manufacturer's instructions.

Statistical analysis

The differences between groups regarding the tumor necrosis area, vascular number, percentage of lymphoma cells in mouse spleen cell suspensions and human sIL2R concentrations in mouse serum were examined with the Mann-Whitney *U* test. All analyses were performed with SPSS Statistics 17.0 (SPSS Inc., Chicago, IL, USA). In this study, $P < 0.05$ was considered significant.

RESULTS

VEGF-A expression in DLBCL

VEGF-A expression by DLBCL cells in the lymph node lesions according to GCB or non-GCB phenotypes are shown in Figure 1a.

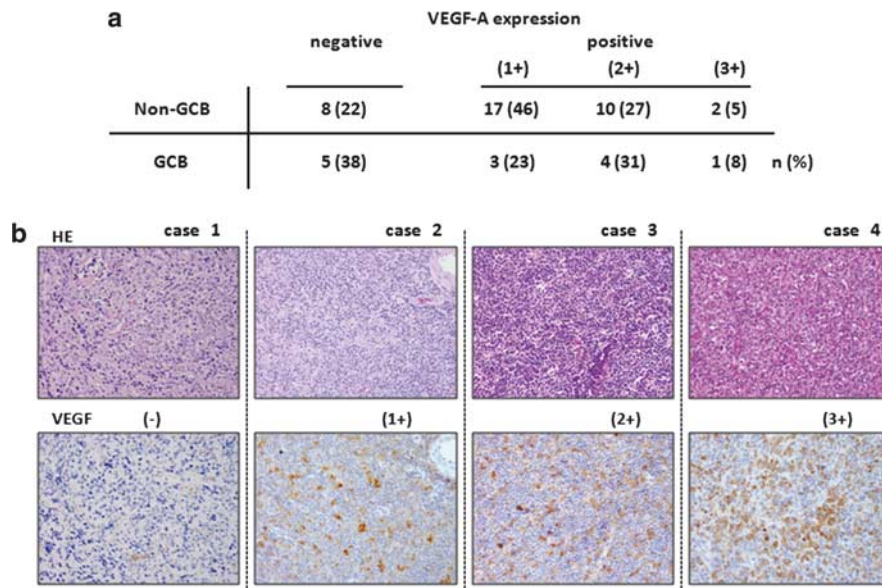


Figure 1. VEGF-A expression in DLBCL. **(a)** VEGF-A expression of DLBCL cells in the lymph node lesions according to GCB or non-GCB phenotypes. VEGF-A expression was categorized based on the percentage of DLBCL cells stained as follows: $\geq 50\%$, 3+ positive; 30–49%, 2+ positive; 10–29%, 1+ positive; $< 10\%$, negative. **(b)** Cases 1, 2, 3 and 4 are representative of VEGF-A negative, 1+, 2+ and 3+ positive categories, respectively. Photomicrographs with hematoxylin and eosin (HE; upper panels) and VEGF-A staining (lower panels) are shown.

Immunopathological features of four cases from each group stratified by VEGF-A expression are shown in Figure 1b. Differences in VEGF-A expression levels between the two DLBCL groups (GCB versus non-GCB) did not achieve significance (Fisher's exact test).

Establishment of the primary DLBCL cell-bearing NOG mouse model

The macroscopic appearance of a primary DLBCL cell-bearing NOG mouse is shown in Figure 2a, demarcating the i.p. mass and splenomegaly by thin white dotted lines. Flow cytometric analysis demonstrated that the mass mainly consisted of human cells expressing CD19 and CD25 (Figure 2b). Immunopathological analysis revealed that it consisted of large atypical cells with irregular and pleomorphic nuclei, and blood vessels. The cells were CD20+, but CD3-negative (Figure 2c). These findings are consistent with DLBCL. The cells were in addition positive for CD25 and negative for EBER (data not shown). VEGF expression was 1+ positive. The DLBCL cells were also positive for MUM1/IRF4, but negative for CD10 and BCL-6 (data not shown), and were thus classified as non-GCB phenotype. These immunopathological findings on the NOG DLBCL cells were identical to those of the donor DLBCL.

Blood vessels in the tumor tissue were stained by anti- α -SMA Ab (Figure 2c). Vascular endothelial cells in the tumor tissue were stained by anti-von Willebrand Factor Ab, but not by anti-CD31 mAb (data not shown). These results indicated that blood vessels in the tumor originated from the mouse, because anti- α -SMA and von Willebrand Factor Ab used in the present study recognized the corresponding protein derived from both human and mice, whereas the anti-CD31 mAb recognized the corresponding human but not murine protein (data not shown).

DLBCL cell infiltration into spleen, liver and bone marrow was seen both by flow cytometry (Figure 2d, upper panels) and pathological analyses (Figure 2d, lower panels).

The tumor cells recovered from mice receiving the primary lymphoma cells were serially i.p. transplanted into other NOG mice. This procedure of transfer from mouse to mouse was repeated successfully until at least the fifth passage. The

macroscopic features of the animals and the immunopathological findings for the tumor changed little through these serial passages. We could passage tumor cells that had been kept frozen until use, as well as those freshly isolated (data not shown). In contrast, these DLBCL cells could not be maintained *in vitro* in culture (data not shown).

VEGF-A, VEGF-R1 and -R2 expression in DLBCL cell lines

VEGF-A mRNA expression was detected in all eight DLBCL cell lines tested and in NOG DLBCL cells from i.p. masses (Figure 3a, left panel). VEGF-R1 mRNA expression was present only in two (OCI-Ly19 and Toledo) of the DLBCL cell lines and in the NOG DLBCL cells (Figure 3a, right panel). No VEGF-R2 mRNA expression was detected in any of the eight DLBCL cell lines tested, or in the NOG DLBCL cells (data not shown). Flow cytometry demonstrated that VEGF-R1 protein was also expressed in the two lines with mRNA (OCI-Ly19 and Toledo, Figure 3b), consistent with the results from reverse transcription PCR. VEGF-R1 expression in NOG DLBCL cells as assessed by flow cytometry was very weak (Figure 3b) and VEGF-R2 was not expressed at all in any of the DLBCL cell lines tested, or in NOG DLBCL cells (data not shown), also consistent with the reverse transcription PCR results.

Bevacizumab-mediated anti-proliferative activity against DLBCL cells *in vitro*

Bevacizumab did not directly block the proliferation of OCI-Ly19 and Toledo cells *in vitro*, despite their expression of both VEGF-A and VEGF-R1 (Figure 3c, upper panels). Neither did it inhibit NOG DLBCL cells, with or without the addition of interleukin-2 (Figure 3c, lower panels).

CHOP + bevacizumab has significantly greater therapeutic efficacy than CHOP alone in primary DLBCL cell-bearing NOG mice

Treatment with CHOP + bevacizumab resulted in an increased percentage of tumor necrosis in the primary DLBCL cell-bearing NOG mice (mean 12.7%, median 11.1%, range 5.2–18.7%), compared with CHOP alone (mean 1.8%, median 1.5%, range 1.0–2.7%, $P = 0.0090$; Figure 4a, left panel). An example of

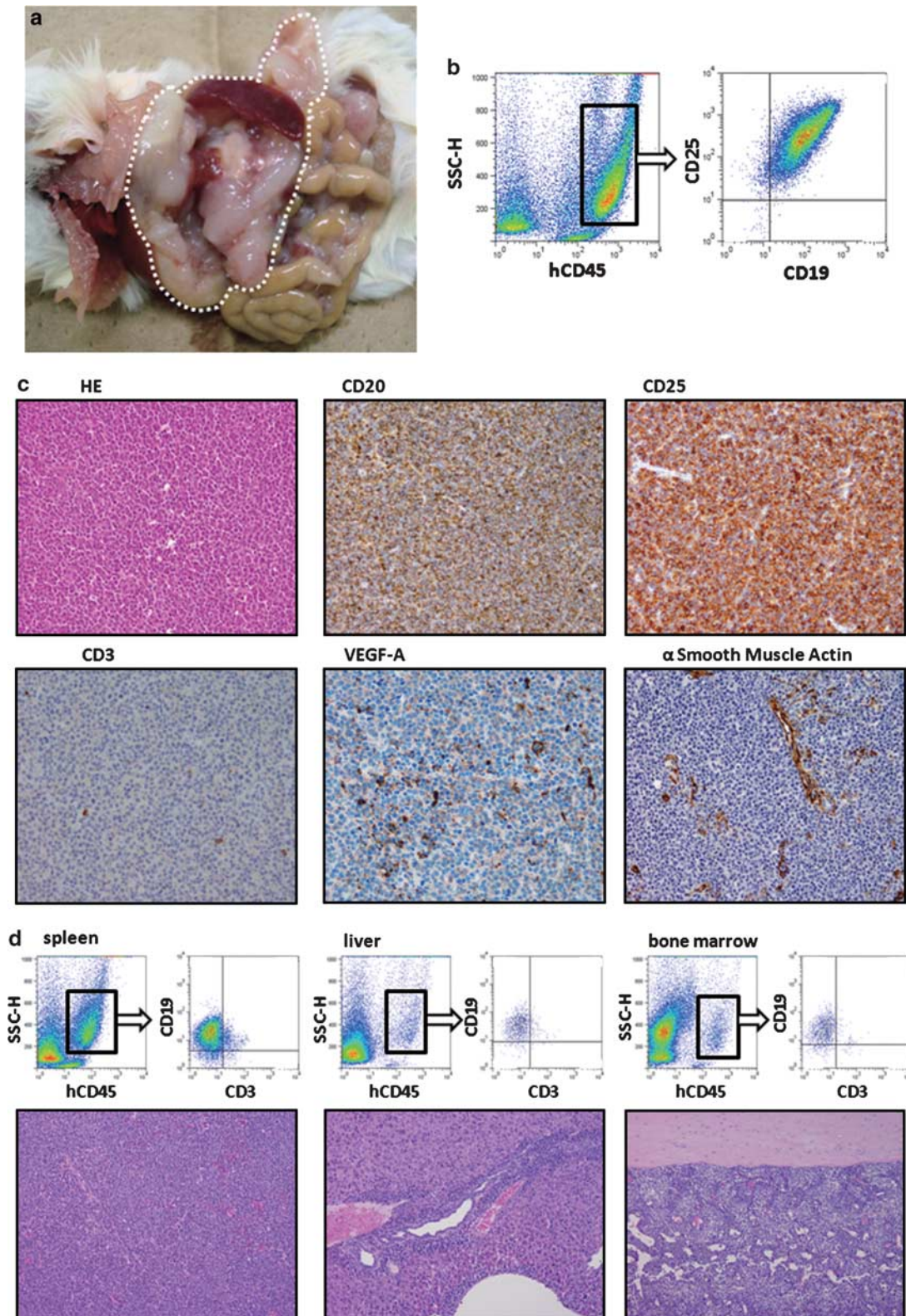


Figure 2. Primary DLBCL cell-bearing NOG mouse model. (a) Macroscopic appearance of a primary DLBCL cell-bearing NOG mouse. The intraperitoneal mass is demarcated by a thin white dotted line. (b) Human CD45⁺ cells in the mass determined by human CD19 and CD25 expression. (c) Immunohistochemical images of the intraperitoneal mass. (d) Human CD45⁺ cells of each organ determined by human CD3 and CD19 expression (upper panels). Photomicrographs with hematoxylin and eosin (HE) staining of each organ (lower panels).

calculating the percentage necrotic area is presented in Figure 4a, right panels. CHOP + bevacizumab treatment resulted in decreased vasculature in the tumor tissues (41.9, 40.9, 32.5–51.3/mm²;

(mean, median, range)), compared with CHOP alone (66.3, 71.8, 40.7–79.5/mm², $P = 0.0472$; Figure 4b, left panel). An example of this calculation is presented in Figure 4b, right-hand panels.

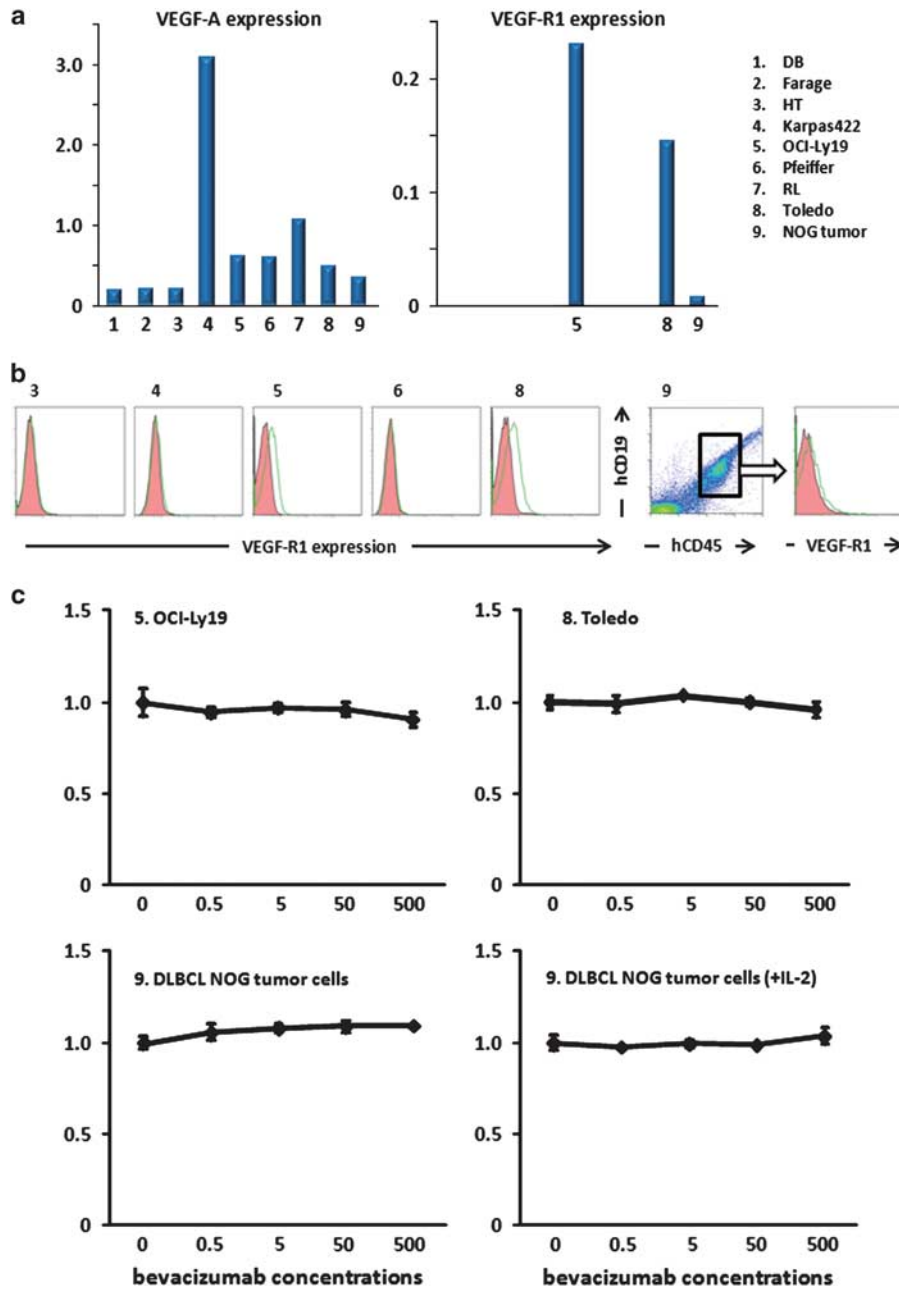


Figure 3. VEGF-A, VEGF-R1 and VEGF-R2 expression in DLBCL cell lines. **(a)** Quantitative reverse transcription (RT)-PCR analysis for VEGF-A and VEGF-R1 in eight DLBCL cell lines, and NOG DLBCL cells from the intraperitoneal mass. **(b)** Flow cytometry for VEGF-R1 in DLBCL cell lines, and NOG DLBCL cells from the intraperitoneal mass. **(c)** Bevacizumab has no direct anti-proliferative activity against DLBCL cell lines (OCI-Ly19 and Toledo) expressing both VEGF-A and VEGF-R1 (upper panels), and NOG DLBCL cells (lower panels), *in vitro*. Each result represents three independent experiments.

As sIL2R appears in the serum, concomitant with its increased expression on cells,²² we measured human sIL2R concentrations as a surrogate marker reflecting the tumor burden of the human CD25-expressing DLBCL. Treatment with CHOP + bevacizumab showed significantly greater therapeutic efficacy as demonstrated by sIL2R concentrations in the primary DLBCL cell-bearing NOG mice ($44.6, 46.1, 28.5\text{--}59.2 \times 10^3$ pg/ml), compared with CHOP alone ($83.5, 78.1, 49.5\text{--}119.3 \times 10^3$ pg/ml, $P = 0.0283$; Figure 4c).

The percentages of DLBCL cells in spleen cell suspensions of CHOP and CHOP + bevacizumab-treated mice were 14.1%, 11.4%, 10.2–20.7%, and 26.1%, 24.6% and 19.0–34.6%, respectively. This difference was statistically significant ($P = 0.0163$; Figure 3d,

left panel). An example of the calculation is shown in Figure 4d, right panels.

Macroscopic and microscopic findings in mice with or without bevacizumab therapy

The appearance of primary DLBCL cell-bearing control mice (treated with saline) or those treated with bevacizumab alone is shown in Figure 5a, upper and lower panels, respectively. Tumor masses are demarcated by thin white dotted lines. Photomicrographs of tumor tissue from each mouse are also shown (Figure 5b).

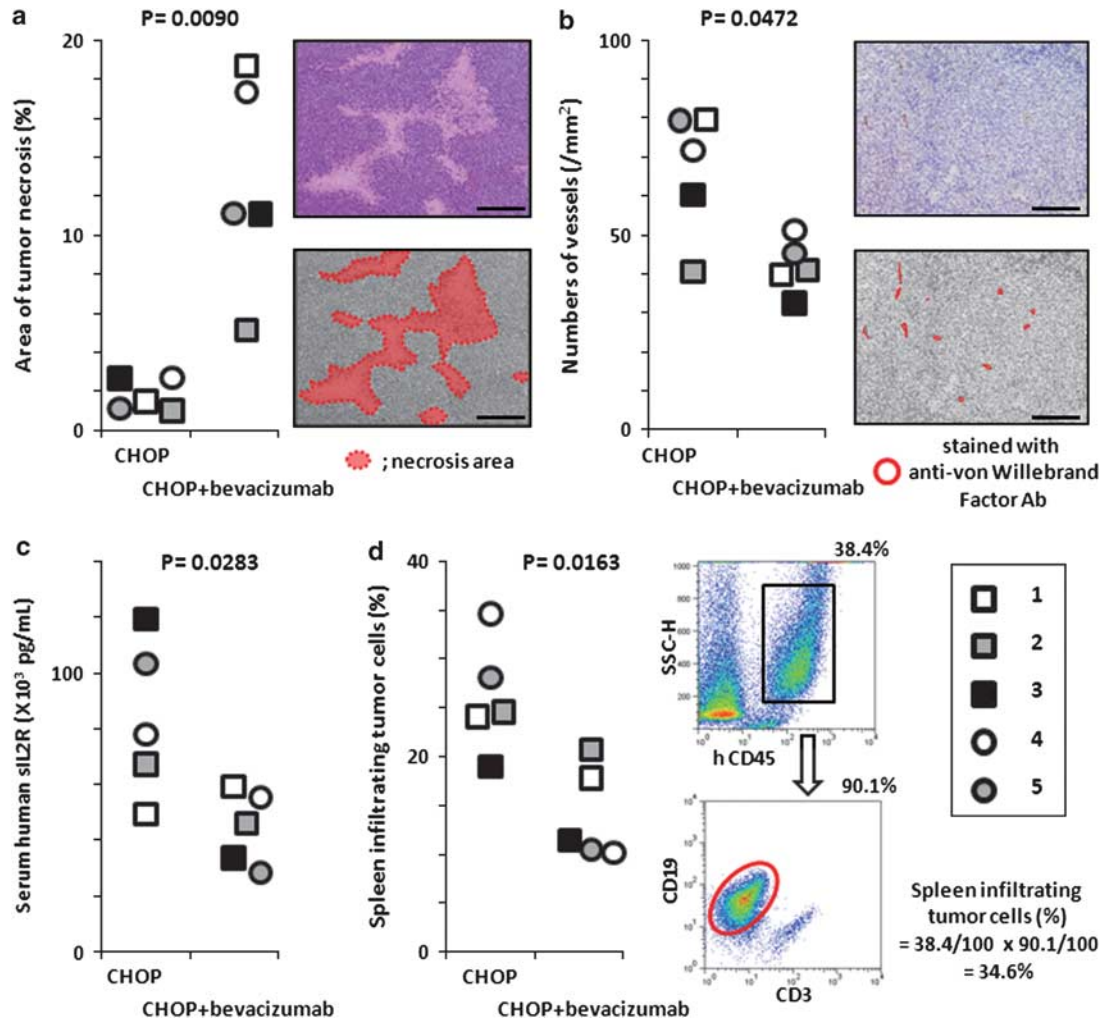


Figure 4. CHOP + bevacizumab has greater therapeutic efficacy than CHOP alone. **(a)** Area of tumor necrosis (%) of each primary DLBCL-bearing NOG mouse. The CHOP + bevacizumab-treated mice had significantly greater tumor necrosis than CHOP-treated mice (left panel). An example of a calculation for tumor necrosis area (%) by means of Image J software is shown (scale bar, 200 μ m; right panels). **(b)** Numbers of vessels (per mm²) of each primary DLBCL-bearing NOG mouse. The CHOP + bevacizumab recipients had significantly fewer than CHOP recipients (left panel). An example of such a calculation by means of Image J software is shown (scale bar, 200 μ m; right panels). **(c)** Serum sIL2R concentrations of each primary DLBCL-bearing NOG mouse. The CHOP + bevacizumab recipients had significantly lower levels of sIL2R than CHOP recipients. **(d)** Spleen-infiltrating tumor cells (%) of each primary DLBCL-bearing NOG mouse. The CHOP + bevacizumab recipients had significantly lower levels of spleen-infiltrating tumor cells than CHOP recipients (left panel). An example of a calculation of spleen-infiltrating tumor cells (%) is shown (right panels).

Bevacizumab therapy alone has significant therapeutic efficacy in primary DLBCL cell-bearing NOG mice.

Treatment with bevacizumab alone significantly increased the percentage tumor necrotic area (7.5, 4.8, 2.1–18.7%) compared with control mice (2.0, 1.7, 0.1–5.6%, $P = 0.0070$; Figure 6a). This was also the case when considering vascularization of the tumor tissues (46.2, 43.1, 33.6–60.0/mm², compared with 66.7, 64.8, 50.1–99.9/mm² in controls, $P = 0.0070$; Figure 6b). Treatment with bevacizumab showed significantly greater therapeutic efficacy as demonstrated by sIL2R concentrations in the primary DLBCL cell-bearing NOG mice (187.6, 185.2, 5.0–350.8 $\times 10^3$ pg/ml), compared with controls (459.6, 482.8, 201.5–689.5 $\times 10^3$ pg/ml, $P = 0.0041$; Figure 6c).

The percentages of DLBCL cells in spleen cell suspensions of bevacizumab- and saline-treated mice were 13.1, 14.6, 0.1–27.5% and 18.7%, 18.8%, 4.0–31.7%, respectively, but this difference was not statistically significant (data not shown).

DISCUSSION

In the present study, we have achieved two goals: first, to establish a novel mouse model using NOG recipients engrafted with primary DLBCL cells from a patient, in which the tumor cells survive and proliferate in a murine microenvironment-dependent manner; second, to document that bevacizumab possesses significant therapeutic efficacy in these primary DLBCL cell-bearing mice.

NOG mice have severe, multiple immune dysfunctions, such that human immune cells engrafted into them retain essentially the same functions as in humans.^{23,24} In the present system, primary DLBCL cells expressing CD19, CD20 and CD25 formed large i.p. masses, and markedly infiltrated into different organs such as spleen, liver and bone marrow. The presented features were very similar to the donor DLBCL patient. The lymphoma cells were positive for VEGF-A and therefore it would be expected that the interaction of VEGF-A produced by tumor cells with VEGF-R2

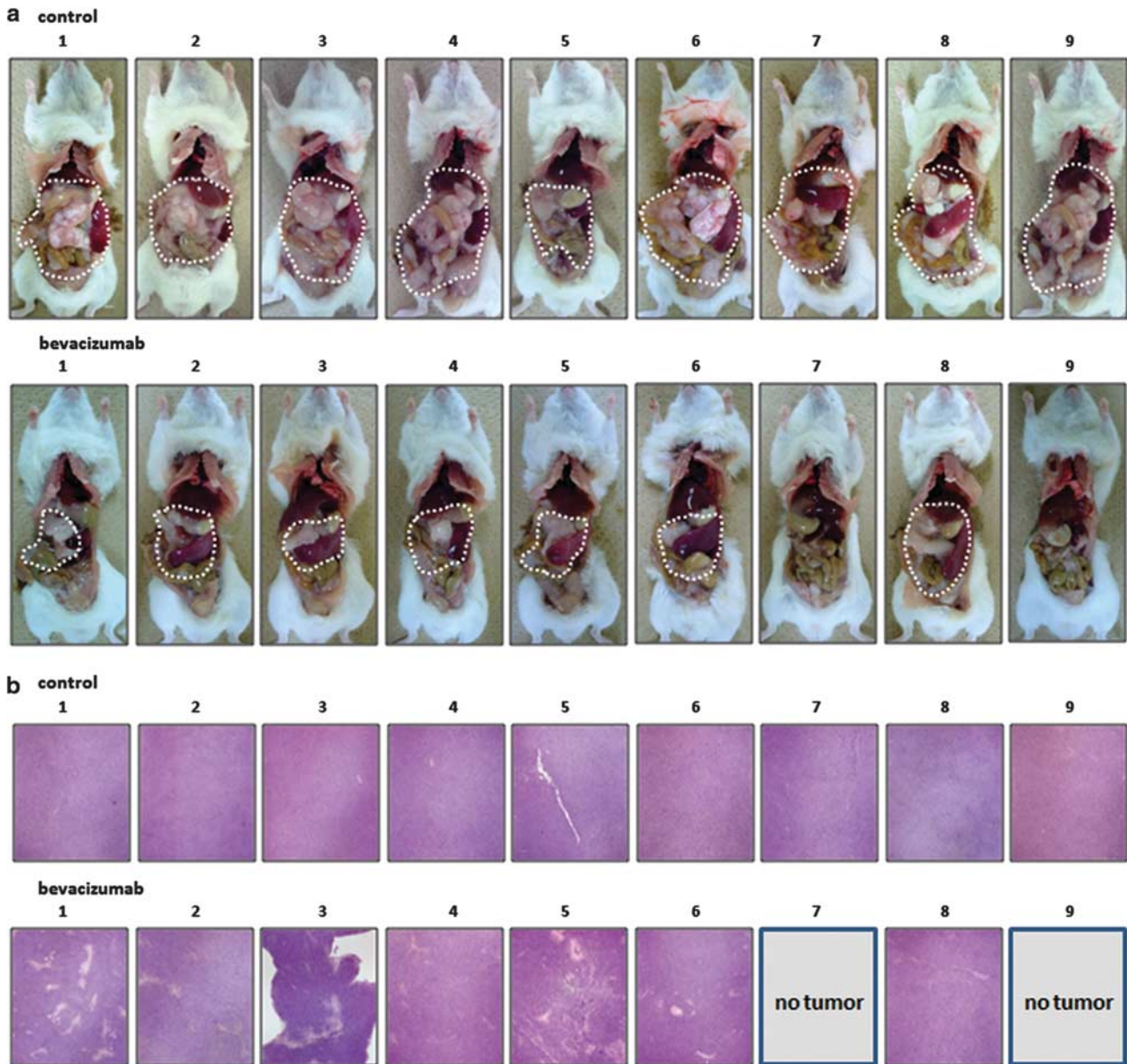


Figure 5. Macroscopic and microscopic findings of mice with or without bevacizumab therapy. (a) Macroscopic appearance of mice treated with saline (control; upper panels) or bevacizumab (lower panels). Tumor masses are demarcated by thin white dotted lines. (b) Photomicrographs with hematoxylin and eosin (HE) staining of saline (control; upper panels) or bevacizumab-treated tumor (lower panels).

on host (mice) endothelial cells should have an important role in tumor angiogenesis, leading to tumor cell survival and proliferation supported by receiving sufficient nutrients and oxygen, as reported by other investigators.^{25–27} To the best of our knowledge, this is the first report of primary DLBCL cell-bearing mice, in which the DLBCL cells can be maintained by serial transplantations, but cannot be maintained *in vitro* in culture. This indicates that the microenvironment is indispensable for tumor survival; thus the present DLBCL model should better reflect the human DLBCL *in vivo* environment, compared with other mouse models using established tumor cell lines. Therefore, this model should provide a powerful tool for understanding the pathogenesis of DLBCL and, furthermore, for the one which can be used not only to evaluate novel cytotoxic anti-DLBCL cell agents, but also antitumor agents targeting the microenvironment, including bevacizumab, more appropriately,

in vivo. The observed significant antitumor activities of bevacizumab combined with CHOP therapy were expected, because bevacizumab is known only to be of benefit to patients with metastatic colorectal, non-small cell lung and metastatic breast cancer, when combined with chemotherapy.^{8–10} The effect observed in mice receiving bevacizumab + CHOP, as demonstrated by the increased tumor necrosis area and reduced vasculature in the tumor tissue, was consistent with the conventional antitumor mechanism of bevacizumab, which neutralizes the human VEGF-A produced by the tumor cells, but not murine VEGF-A.²⁸ It then inhibits the growth of new blood vessels and thus starves tumor cells of necessary nutrients and oxygen.²⁹ This should lead to a reduced tumor burden, as indicated by the sIL2R concentrations measured. It was also reported that lymphoma cell growth was promoted in an autocrine manner via VEGF-A/VEGF-R1 or VEGF-A/VEGF-R2

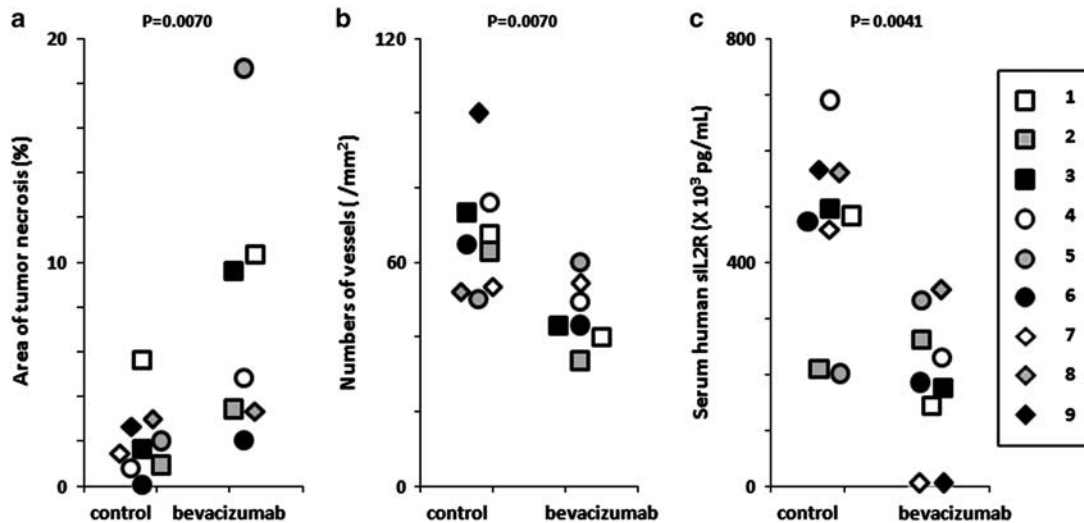


Figure 6. Bevacizumab therapy has significant therapeutic efficacy in the DLBCL mice. **(a)** Area of tumor necrosis (%) of each primary DLBCL-bearing NOG mouse. The bevacizumab-treated mice had significantly more tumor necrosis than controls. **(b)** Vessel numbers (per mm²) of each primary DLBCL-bearing NOG mouse. The bevacizumab recipients had significantly fewer vessel numbers than controls. **(c)** Serum sIL2R concentrations of each primary DLBCL-bearing NOG mouse. The bevacizumab recipients had significantly lower levels of sIL2R than controls.

interactions,²⁵ but the present *in vitro* data did not support that observation. In the present study, significant effects of bevacizumab alone were also observed, as demonstrated by the increased area of tumor necrosis and reduced vasculature in the tumor tissue, leading to a degree of antitumor therapeutic efficacy as demonstrated by reduced tumor burden indicated by serum sIL2R concentrations. In contrast to combination therapy, bevacizumab alone was not active when assessed by the percentages of DLBCL cells in the spleen. One possible explanation for this is that the spleen is likely to be more richly vascularized compared with the tumor mass, and thus bevacizumab alone has little starvation effect on the tumor cells therein. It has been reported that VEGF-targeted therapy can 'normalize' the tumor vascular network and that this can lead to a more uniform blood-flow, with subsequent increased delivery of chemotherapeutic agents.^{30–32} Therefore, the tumor cells in spleen might be efficiently reduced only when bevacizumab is combined with chemotherapy.

The present study demonstrated the importance of angiogenesis for the pathogenesis of VEGF-expressing DLBCL. Ganjoo *et al.*³³ reported that VEGF expression was detected in 42–60% of tumor cells in DLBCL and Gratzinger *et al.*³⁴ found that 60% of cases showed strong VEGF immunoreactivity, defined as VEGF expression in >30% of the tumor cells. These reports together with our present study indicate that targeting angiogenesis would be a promising strategy for at least a subgroup of DLBCL patients whose tumors depend to a large extent on angiogenesis via VEGF for survival and proliferation. In fact, bevacizumab as a single agent has been reported to have modest clinical activity in patients in the setting of relapsed aggressive non-Hodgkin lymphoma³⁵ and in combination with rituximab-CHOP in first-line treatment.³³ However, a phase III clinical study evaluating the efficacy and safety of bevacizumab together with rituximab plus CHOP in patients with DLBCL (MAIN trial) could not be completed after a safety and efficacy analysis of the first 720 patients. We believe that this result of the MAIN trial does not necessarily have to lead to the conclusion that bevacizumab is ineffective in DLBCL. Analogously, the epidermal growth factor receptor tyrosine kinase inhibitor, gefitinib, failed to yield a significantly improved overall survival in patients with refractory non-small cell lung cancer,³⁶ but did show therapeutic benefit in a subgroup of patients with mutated epidermal growth factor receptor.^{37–39} In the case of

mAb targeting the epidermal growth factor receptor, both panitumumab and cetuximab also provide clinical benefits only to a subgroup of colorectal cancer patients with wild-type *KRAS* and *BRAF*.⁴⁰ These findings indicate that we should develop novel treatment strategies based on tumor biology and not on tumor category. DLBCL is a highly heterogeneous category with respect to biology, morphology and clinical presentation,¹⁶ as are non-small cell lung cancer or colorectal cancer. Therefore, further investigations are warranted to determine which subgroups of DLBCL patients will benefit from bevacizumab therapy.

In conclusion, using NOG mice as recipients, we have established a novel model in which primary DLBCL cells from a patient engraft and proliferate in a murine microenvironment-dependent manner. The present DLBCL model should more truly reproduce the human DLBCL *in vivo* environment, compared with any other current models, which use established tumor cell lines. This is the first report to evaluate the efficacy of bevacizumab in such a tumor microenvironment-dependent model. Bevacizumab therapy could be a potential treatment strategy for that subgroup of DLBCL depending to a large extent on angiogenesis via VEGF for tumor survival and proliferation.

CONFLICT OF INTEREST

The authors declare no conflict of interest.

ACKNOWLEDGEMENTS

We thank Ms Chiori Fukuyama for her excellent technical assistance. Grants-in-aid for (a) Young Scientists (no. 22689029: T Ishida) and (b) Scientific Research (no. 22300333: T Ishida and R Ueda), and Scientific Support Programs for Cancer Research (no. 22150001, T Ishida) from the Ministry of Education, Culture, Sports, Science and Technology of Japan; Grants-in-aid for National Cancer Center Research and Development Fund (no. 21-6-3: T Ishida); and Health and Labour Sciences Research Grants (H22-Clinical Cancer Research-general-028: T Ishida and H23-Third Term Comprehensive Control Research for Cancer-general-011: T Ishida and H Inagaki) from Ministry of Health, Labour and Welfare, Japan.

REFERENCES

- Sautès-Fridman C, Cherfils-Vicini J, Damotte D, Fisson S, Fridman WH, Cremer I *et al.* Tumor microenvironment is multifaceted. *Cancer Metastasis Rev* 2011; **30**: 13–25.

- 2 Folkman J. Angiogenesis: an organizing principle for drug discovery? *Nat Rev Drug Discov* 2007; **6**: 273–286.
- 3 Kim KJ, Li B, Winer J, Armanini M, Gillett N, Phillips HS et al. Inhibition of vascular endothelial growth factor-induced angiogenesis suppresses tumour growth *in vivo*. *Nature* 1993; **362**: 841–844.
- 4 Ferrara N, Hillan KJ, Gerber HP, Novotny W. Discovery and development of bevacizumab, an anti-VEGF antibody for treating cancer. *Nat Rev Drug Discov* 2004; **3**: 391–400.
- 5 Ito M, Hiramatsu H, Kobayashi K, Suzue K, Kawahata M, Hioki K et al. NOD/SCID/ γ cnll mouse: an excellent recipient mouse model for engraftment of human cells. *Blood* 2002; **100**: 3175–3182.
- 6 Ito M, Kobayashi K, Nakahata T. NOD/Shi-scid IL2r γ null (NOG) mice more appropriate for humanized mouse models. *Curr Top Microbiol Immunol* 2008; **324**: 53–76.
- 7 Yang JC, Haworth L, Sherry RM, Hwu P, Schwartzentruber DJ, Topalian SL et al. A randomized trial of bevacizumab, an anti-vascular endothelial growth factor antibody, for metastatic renal cancer. *N Engl J Med* 2003; **349**: 427–434.
- 8 Hurwitz H, Fehrenbacher L, Novotny W, Cartwright T, Hainsworth J, Heim W et al. Bevacizumab plus irinotecan, fluorouracil, and leucovorin for metastatic colorectal cancer. *N Engl J Med* 2004; **350**: 2335–2342.
- 9 Sandler A, Gray R, Perry MC, Brahmer J, Schiller JH, Dowlati A et al. Paclitaxel-carboplatin alone or with bevacizumab for non-small-cell lung cancer. *N Engl J Med* 2006; **355**: 2542–2550.
- 10 Miller K, Wang M, Gralow J, Dickler M, Cobleigh M, Perez EA et al. Paclitaxel plus bevacizumab versus paclitaxel alone for metastatic breast cancer. *N Engl J Med* 2007; **357**: 2666–2676.
- 11 Vredenburgh JJ, Desjardins A, Herndon 2nd JE, Marcello J, Reardon DA, Quinn JA et al. Bevacizumab plus irinotecan in recurrent glioblastoma multiforme. *J Clin Oncol* 2007; **25**: 4722–4729.
- 12 Saltz LB, Clarke S, Díaz-Rubio E, Scheithauer W, Figuer A, Wong R et al. Bevacizumab in combination with oxaliplatin-based chemotherapy as first-line therapy in metastatic colorectal cancer: a randomized phase III study. *J Clin Oncol* 2008; **26**: 2013–2019.
- 13 Hochster HS, Hart LL, Ramanathan RK, Childs BH, Hainsworth JD, Cohn AL et al. Safety and efficacy of oxaliplatin and fluoropyrimidine regimens with or without bevacizumab as first-line treatment of metastatic colorectal cancer: results of the TREE Study. *J Clin Oncol* 2008; **26**: 3523–3529.
- 14 Reck M, von Pawel J, Zatlok P, Ramlau R, Gorbounova V, Hirsh V et al. Phase III trial of cisplatin plus gemcitabine with either placebo or bevacizumab as first-line therapy for nonsquamous non-small-cell lung cancer: AVAIL. *J Clin Oncol* 2009; **27**: 1227–1234.
- 15 Miles DW, Chan A, Dirix LY, Cortés J, Pivrot X, Tomczak P et al. Phase III study of bevacizumab plus docetaxel compared with placebo plus docetaxel for the first-line treatment of human epidermal growth factor receptor 2-negative metastatic breast cancer. *J Clin Oncol* 2010; **28**: 3239–3247.
- 16 Nogai H, Dörken B, Lenz G. Pathogenesis of non-Hodgkin's lymphoma. *J Clin Oncol* 2011; **29**: 1803–1811.
- 17 A clinical evaluation of the International Lymphoma Study Group classification of non-Hodgkin's lymphoma. The Non-Hodgkin's Lymphoma Classification Project. *Blood* 1997; **89**: 3909–3918.
- 18 Hans CP, Weisenburger DD, Greiner TC, Gascoyne RD, Delabie J, Ott G et al. Confirmation of the molecular classification of diffuse large B-cell lymphoma by immunohistochemistry using a tissue microarray. *Blood* 2004; **103**: 275–282.
- 19 Abramoff MD, Magelhaes PJ, Ram SJ. Image Processing with ImageJ. *Biophotonics Int* 2004; **11**: 36–42.
- 20 Ishida T, Iida S, Akatsuka Y, Ishii T, Miyazaki M, Komatsu H et al. The CC chemokine receptor 4 as a novel specific molecular target for immunotherapy in adult T-Cell leukemia/lymphoma. *Clin Cancer Res* 2004; **10**: 7529–7539.
- 21 Mohammad RM, Wall NR, Dutcher JA, Al-Katib AM. The addition of bryostatin 1 to cyclophosphamide, doxorubicin, vincristine, and prednisone (CHOP) chemotherapy improves response in a CHOP-resistant human diffuse large cell lymphoma xenograft model. *Clin Cancer Res* 2000; **6**: 4950–4956.
- 22 Waldmann TA. The IL-2/IL-2 receptor system: a target for rational immune intervention. *Immunol Today* 1993; **14**: 264–270.
- 23 Ito A, Ishida T, Yano H, Inagaki A, Suzuki S, Sato F et al. Defucosylated anti-CCR4 monoclonal antibody exercises potent ADCC-mediated antitumor effect in the novel tumor-bearing humanized NOD/Shi-scid, IL-2R γ gamma(null) mouse model. *Cancer Immunol Immunother* 2009; **58**: 1195–1206.
- 24 Ito A, Ishida T, Utsunomiya A, Sato F, Mori F, Yano H et al. Defucosylated anti-CCR4 monoclonal antibody exerts potent ADCC against primary ATLL cells mediated by autologous human immune cells in NOD/Shi-scid, IL-2R γ gamma(null) mice *in vivo*. *J Immunol* 2009; **183**: 4782–4791.
- 25 Wang ES, Teruya-Feldstein J, Wu Y, Zhu Z, Hicklin DJ, Moore MA. Targeting autocrine and paracrine VEGF receptor pathways inhibits human lymphoma xenografts *in vivo*. *Blood* 2004; **104**: 2893–2902.
- 26 Borgström P, Hillan KJ, Sriramarao P, Ferrara N. Complete inhibition of angiogenesis and growth of microtumors by anti-vascular endothelial growth factor neutralizing antibody: novel concepts of angiostatic therapy from intravital videomicroscopy. *Cancer Res* 1996; **56**: 4032–4039.
- 27 Ruan J, Hajjar K, Rafii S, Leonard JP. Angiogenesis and antiangiogenic therapy in non-Hodgkin's lymphoma. *Ann Oncol* 2009; **20**: 413–424.
- 28 Yu L, Wu X, Cheng Z, Lee CV, LeCouter J, Campa C et al. Interaction between bevacizumab and murine VEGF-A: a reassessment. *Invest Ophthalmol Vis Sci* 2008; **49**: 522–527.
- 29 Ellis LM, Hicklin DJ. VEGF-targeted therapy: mechanisms of anti-tumour activity. *Nat Rev Cancer* 2008; **8**: 579–591.
- 30 Jain RK. Normalization of tumor vasculature: an emerging concept in antiangiogenic therapy. *Science* 2005; **307**: 58–62.
- 31 Gerber HP, Ferrara N. Pharmacology and pharmacodynamics of bevacizumab as monotherapy or in combination with cytotoxic therapy in preclinical studies. *Cancer Res* 2005; **65**: 671–680.
- 32 Carmeliet P, Jain RK. Principles and mechanisms of vessel normalization for cancer and other angiogenic diseases. *Nat Rev Drug Discov* 2011; **10**: 417–427.
- 33 Ganjoo KN, An CS, Robertson MJ, Gordon LI, Sen JA, Weisenbach J et al. Rituximab, Bevacizumab and CHOP (RA-CHOP) in untreated diffuse large B-cell lymphoma: safety, biomarker and pharmacokinetic analysis. *Leuk Lymphoma* 2006; **47**: 998–1005.
- 34 Gratzinger D, Zhao S, Marinelli RJ, Kapp AV, Tibshirani RJ, Hammer AS et al. Microvessel density and expression of vascular endothelial growth factor and its receptors in diffuse large B-cell lymphoma subtypes. *Am J Pathol* 2007; **170**: 1362–1369.
- 35 Stopeck AT, Unger JM, Rimsza LM, Bellamy WT, Iannone M, Persky DO et al. A phase II trial of single agent bevacizumab in patients with relapsed, aggressive non-Hodgkin lymphoma: Southwest oncology group study S0108. *Leuk Lymphoma* 2009; **50**: 728–735.
- 36 Thatcher N, Chang A, Parikh P, Rodrigues Pereira J, Ciuleanu T, von Pawel J et al. Gefitinib plus best supportive care in previously treated patients with refractory advanced nonsmall-cell lung cancer: results from a randomised, placebo-controlled, multicentre study (Iressa Survival Evaluation in Lung Cancer). *Lancet* 2005; **366**: 1527–1537.
- 37 Maemondo M, Inoue A, Kobayashi K, Sugawara S, Oizumi S, Isobe H et al. Gefitinib or chemotherapy for non-small-cell lung cancer with mutated EGFR. *N Engl J Med* 2010; **362**: 2380–2388.
- 38 Lynch TJ, Bell DW, Sordella R, Gurubhagavatula S, Okimoto RA, Brannigan BW et al. Activating mutations in the epidermal growth factor receptor underlying responsiveness of non-small-cell lung cancer to gefitinib. *N Engl J Med* 2004; **350**: 2129–2139.
- 39 Paez JG, Janne PA, Lee JC, Tracy S, Greulich H, Gabriel S et al. EGFR mutations in lung cancer: correlation with clinical response to gefitinib therapy. *Science* 2004; **304**: 1497–1500.
- 40 Bardelli A, Siena S. Molecular mechanisms of resistance to cetuximab and panitumumab in colorectal cancer. *J Clin Oncol* 2010; **28**: 1254–1261.



This work is licensed under the Creative Commons Attribution-NonCommercial-No Derivative Works 3.0 Unported License. To view a copy of this license, visit <http://creativecommons.org/licenses/by-nc-nd/3.0/>